Metal-Containing Inhibitors

DOI: 10.1002/anie.201307849

# An Organometallic Inhibitor for the Human Repair Enzyme 7,8-Dihydro-8-oxoguanosine Triphosphatase**

*Manuel Streib, Katja Kräling, Kristin Richter, Xiulan Xie, Holger Steuber,* and Eric Meggers**

***Abstract:*** *The probe-based discovery of the first small-molecule inhibitor of the repair enzyme 8-oxo-dGTPase (MTH1) is presented, which is an unconventional cyclometalated ruthenium half-sandwich complex. The organometallic inhibitor with low-nanomolar activity displays astonishing specificity, as verified in tests with an extended panel of protein kinases and other ATP binding proteins. The binding of the organometallic inhibitor to MTH1 is investigated by protein crystallography.*

A significant portion of all proteins encoded in the human genome bind or utilize purine-based nucleosides or nucleotides, such as ATP, GTP, NAD(P), FAD, PAPS, and coenzyme A.[1] These proteins, which include important classes of enzymes such as kinases, ATPases, ligases, helicases, and chaperones, are involved in all types of cellular processes and are at the origin of many human diseases, and therefore constitute important targets for the design of small-molecule drugs. Our group recently introduced a strategy for designing highly potent and selective ATP-mimetic inhibitors of protein kinases based on substitutionally inert transition-metal complexes,[2,3] and we were wondering whether—due to certain common features of nucleotide binding sites[4]—inert transition-metal complexes may constitute an attractive class of scaffolds for the development of inhibitors of other nucleotide binding proteins. We report herein how we have developed a novel organoruthenium complex as the first low-nanomolar and selective inhibitor of the human repair enzyme 7,8-dihydro-8-oxoguanosine triphosphatase (8-oxo-dGTPase, NUDT1, MTH1), an enzyme that hydrolyzes oxidized purine nucleoside triphosphates and thereby prevents their misincorporation into DNA.[5]

We started our study with the design of the organoruthenium half-sandwich complex **1**, which contains a bidentate 8-(pyridin-2-yl)adenine ligand, an $\eta^5$-coordinated cyclopentadienyl moiety, and a CO ligand (Figure 1). Since it possesses a ruthenium-coordinated adenine nucleobase and a molecular structure that is devised to mimic the overall shape of nucleotides, we envisioned that organometallic complex **1** could serve as a probe for adenine nucleotide binding proteins. To verify this hypothesis, a probe-based technology was employed using a biotinylated acyl phosphate derivative of ATP and ADP that can irreversibly react with conserved lysine residues in the pocket of ATP binding proteins; in this way it is possible to determine direct competition between probe and inhibitor binding within any biological sample.[6] Accordingly, when organometallic complex **1** was profiled at a concentration of 100 μM against more than 150 ATP-binding proteins within the lysate of HL60 cells,[7] **1** was identified to be a binder to a few cellular proteins, particularly the nuclear chaperone midasin and a homologue thereof,[8] a protein involved in the pyrimidine biosynthesis (CAD protein),[9] and the repair enzyme MTH1[5] (Figure 2). We chose MTH1 for further investigations since it plays an important role as a repair enzyme related to oxidative stress in cells. Its inhibition might

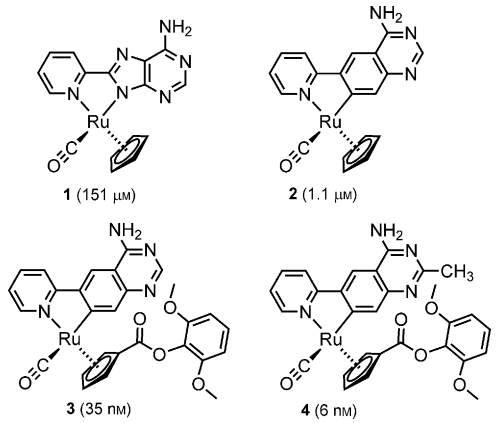


***Figure 1.*** Organometallic complexes investigated and developed as inhibitors for human 8-oxo-dGTPase (MTH1, NUDT1). Determined $IC_{50}$ values are given in brackets. All complexes were synthesized and used as racemates.

[*] M. Streib, K. Kräling, K. Richter, Dr. X. Xie, Prof. Dr. E. Meggers
Fachbereich Chemie, Philipps-Universität Marburg
Hans-Meerwein-Strasse, 35043 Marburg (Germany)
E-mail: meggers@chemie.uni-marburg.de
Dr. H. Steuber[+]
LOEWE-Zentrum für Synthetische Mikrobiologie
Philipps-Universität Marburg
Hans-Meerwein-Strasse, 35043 Marburg (Germany)
Prof. Dr. E. Meggers
College of Chemistry and Chemical Engineering
Xiamen University, Xiamen 361005 (P. R. China)
[+] Current address:
Bayer Pharma AG, Lead Discovery Berlin – Structural Biology
Müllerstrasse 178, 13353 Berlin (Germany)
E-mail: holger.steuber@bayer.com

[**] This work was funded by the German Research Foundation (ME 1805/9-1) and the U.S. National Institutes of Health (CA114046). A generous gift of the MTH1 expression vector from Pär Nordlund (Structural Genomics Consortium) is gratefully acknowledged. We thank the staff of the Bessy MX department for providing beamtime, equipment, and support for data collection. We thank the Helmholtz-Zentrum Berlin (HZB) for synchrotron travel grants.

Supporting information for this article is available on the WWW under http://dx.doi.org/10.1002/anie.201307849.

  

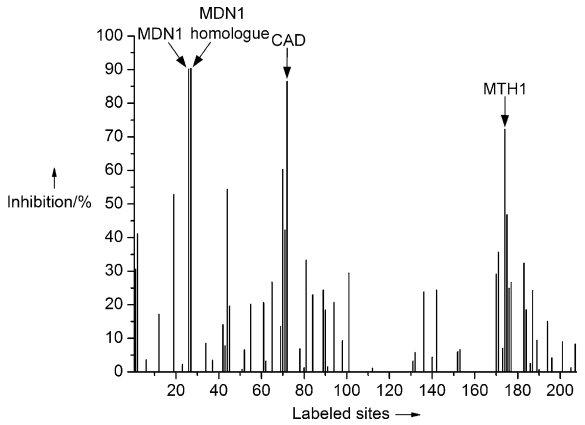


***Figure 2.*** Profiling of complex **1** (100 μM) against ATP binding proteins within the cell lysate of HL60 cells with probe technology (KiNativ, ActivX Biosciences, La Jolla, CA, USA) using a biotinylated acyl phosphate derivative of ATP and ADP. Shown is the inhibition of probe binding by complex **1** to 207 confirmed sites of 153 ATP binding proteins. Main hits: Midasin (MDN1, 90% inh.), a midasin homologue (90% inh.), CAD protein (87% inh.), and 8-oxo-dGTPase (MTH1/NUDT1, 72% inh.). See the Supporting Information for more details.

represent an interesting way to reduce cancer growth since this would result in RAS-induced oxidative damage, leading to DNA double-strand-breaks, and provoking cells to enter premature senescence.[5] Furthermore, the cocrystal structure of MTH1 with bound 8-oxo-dGMP has been reported, thereby potentially facilitating the identification of important inhibitor–enzyme interactions for further improvements of affinity.[10,11]

The concentration of **1** at which the activity of MTH1 is reduced to 50% ($IC_{50}$ value) was determined with an HPLC assay to be a reasonable starting point with a modest value of 151 μM (Figure 3). It is noteworthy that in addition to its affinity for 8-oxo-dGTP ($K_m = 15.2$ μM), MTH1 also binds and efficiently hydrolyzes oxidized ATP derivatives (e.g. 8-oxo-dATP: $K_m = 13.9$ μM),[12] thus rationalizing why the adenine-containing nucleotide probe **1** also binds 8-oxo-dGTPase. Interestingly, when we replaced the 8-(pyridin-2-yl)adenine ligand of **1** with a cyclometalated 4-amino-6-(pyridin-2-yl)quinazoline, the $IC_{50}$ value of the resulting complex **2** was improved by more than two orders of magnitude to 1.1 μM. In a subsequent structure–activity relationship study with this metallo-quinazoline lead structure, the cyclopentadienyl moiety was derivatized and the resulting complex **3** displayed a further improved $IC_{50}$ value of 35 nM (see the Supporting Information for additional derivatives). Finally, the introduction of a methyl group at position 2 of the quinazoline moiety provided a single-digit-nanomolar inhibitor for MTH1 ($IC_{50} = 6$ nM for complex **4**). Compared with the initial probe **1**, the organometallic inhibitor **4** displays an improved affinity for MTH1 by a factor of around 25000.

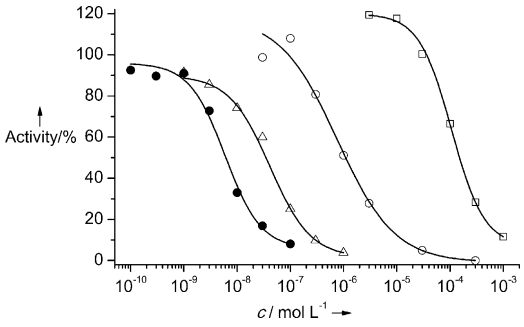


***Figure 3.*** Plot of the inhibition of complexes **1**–**4** against MTH1: **1** = empty squares, **2** = empty circles, **3** = empty triangles, **4** = filled circles. Assay conditions: Compounds **1**–**4** were preincubated with purified MTH1 (10 nM) for 30 min. After addition of 8-oxo-dGTP (25 μM) and incubation for 10 min at 37°C with shaking, the reaction was quenched and analyzed by HPLC to quantify the starting material 8-oxo-dGTP and the product 8-oxo-dGMP.

To understand the binding of the organometallic **4** to MTH1, we cocrystallized racemic **4** with MTH1 and solved the structure to a resolution of 2.70 Å (Table 1).[13] Figure 4 shows the overall structure. As a member of the Nudix hydrolase superfamily,[14] MTH1 exhibits the typical Nudix

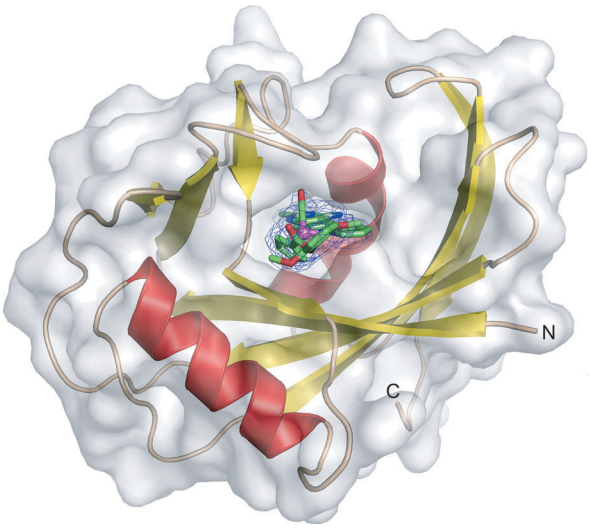


***Figure 4.*** Cocrystal structure of MTH1 (chain A, semitransparent surface view) with the organoruthenium compound (*S*)-**4** bound to the nucleotide binding site. The absolute configuration of the inhibitor was elucidated from its electron density distribution (shown as blue mesh). The SIGMAA-weighted $2F_{obs}-F_{calc}$ difference electron density map of the inhibitor was contoured at 1 $\sigma$.

fold with an arrangement of a mixed β-sheet surrounded by two α-helixes, which along with several loops creates the active site. As expected, the organometallic complex **4** occupies the 8-oxo-dGTP binding site and the electron density distribution, especially of the phenolic ester moiety, allows a clear assignment of the *S* configuration at the stereogenic metal center.[15] As evident in the semitransparent surface view in Figure 4, complex **4** is tightly surrounded by residues from the α-helices, β-sheets, and loops to provide an interaction surface area of approximately 501 $Å^2$.[16] The quinazoline moiety forms several hydrogen bonds, one between the exocyclic $NH_2$ group and Asp119 and one between the endocyclic N3 and Asp120; in addition the endocyclic N1 is in hydrogen-bonding distance to the back-

  

***Table 1:*** Crystallographic data and refinement statistics for **4**/MTH1 (PDB ID: 3WHW).

| | |
|---|---|
| Data collection and Processing | |
| no. of crystals used | 1 |
| wavelength [Å] | 0.91841 |
| space group | $P2_12_12_1$ |
| Unit cell parameters | |
| *a*, *b*, *c* [Å] | 59.76, 67.65, 79.54 |
| α, β, γ [°] | 90, 90, 90 |
| Matthews coefficient [Å$^3$/Da] | 2.21 |
| Solvent content [%] | 44.2 |
| Diffraction data | |
| resolution range [Å] | 25.0–2.70 (2.90-2.70) |
| unique reflections | 9264 (1737) |
| $R(I)_{sym}$ [%] | 16.0 (63.3) |
| completeness [%] | 99.6 (99.0) |
| redundancy | 5.8 (5.7) |
| $I/\sigma(I)$ | 10.62 (3.0) |
| Refinement | |
| resolution range [Å] | 25.0–2.70 |
| reflections used in refinement (work/free) | 8800/464 |
| final *R* values for all reflections (work/free) [%] | 21.5/26.6 |
| Protein residues | 308 |
| Inhibitor atoms | 78 |
| Water molecules | 34 |
| Sulfate ions | 7 |
| RMSDs | |
| bonds [Å] | 0.0085 |
| angles [°] | 1.280 |
| Ramachandran plot | |
| residues in most favored regions [%] | 89.6 |
| residues in additional allowed regions [%] | 10.4 |
| residues in generously allowed regions [%] | – |
| Mean B factor [Å$^2$] | |
| protein | 51.9 |
| inhibitor | 58.9 |
| water molecules | 33.4 |
| sulfate ions | 99.8 |

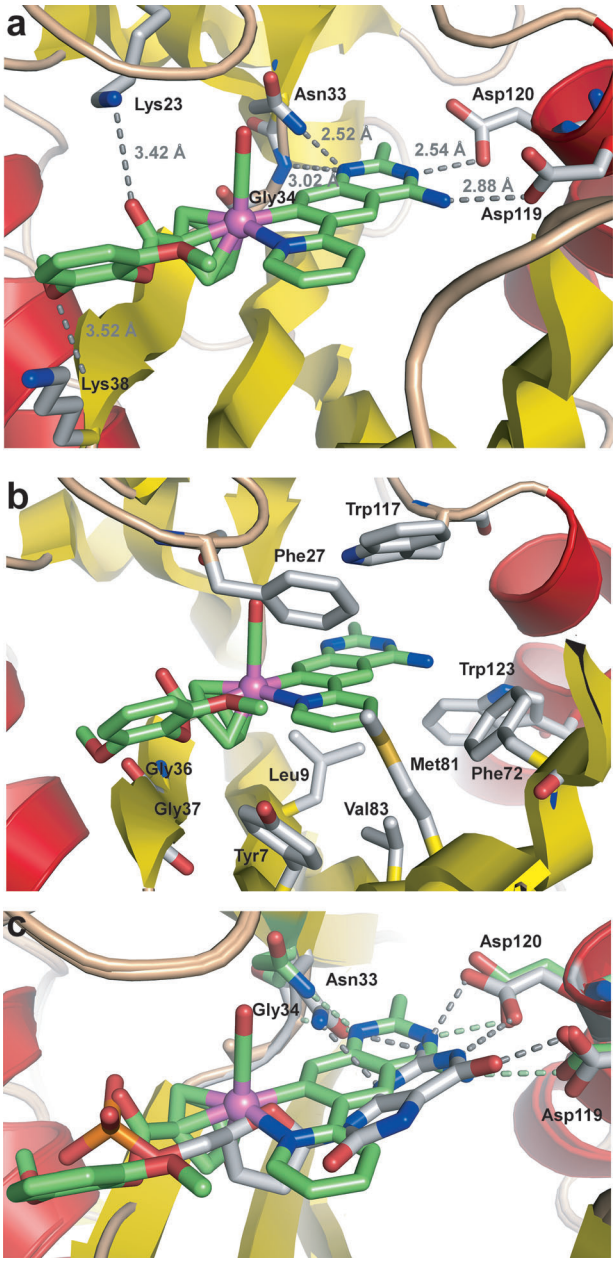


***Figure 5.*** Interactions of (*S*)-**4** with the active-site residues of MTH1 and superimposed cocrystal structures of (*S*)-**4** (green) and 8-oxo-dGMP (gray) with MTH1 (PDB ID: 3ZR0). Alignment was accomplished with PyMOL Molecular Graphics System, Version 0.99rc6, Schrödinger, LLC.

bone NH group of Gly34 and the amide side chain of Asn33 (Figure 5a). Further polar contacts at a larger distance can be identified between the ester carbonyl group of **4** and Lys23, and between a methoxy group of **4** and the backbone NH group of Lys38. The inhibitor is in van der Waals contact with multiple side chains, as highlighted in Figure 5b. Especially intriguing are the number of aromatic side chains stacking face-to-face (Trp117 and Phe27) and edge-to-face (Trp123, Phe72, Tyr7) with the quinazoline ligand of the inhibitor. In order to compare this structure with the binding of (*S*)-**4** with 8-oxo-dGMP (PDB ID: 3ZR0[10]), the two cocrystal structures were superimposed. As displayed in Figure 5c, the pyridyl-quinazoline moiety of (*S*)-**4** colocates roughly with the guanine nucleobase of 8-oxo-dGMP and the ruthenium center aligns with the ribose unit, whereas the 2,6-dimethoxyphenylester fills the space occupied by the phosphate of 8-oxo-dGMP. Although the heteroaromatic quinazoline moiety is somewhat shifted and tilted compared to the purine nucleobase of 8-oxo-dGMP, the same key residues are involved in hydrogen bonding to both ligands, which is possible since the guanine base of 8-oxo-dGMP apparently adopts the lactim tautomeric form.[10]

Overall, the high affinity of (*S*)-**4** to MTH1 can be rationalized by a combination of several hydrogen-bonding interactions, a large number of close van der Waals contacts, and a good match between the shape of the nucleotide binding site and the structure of the organometallic inhibitor. The limited conformational flexibility of **4** not only provides

  

an entropic advantage, which is reflected in the high binding affinity to MTH1, but also contributes to an impressive specificity. In fact, the organometallic compound **4** does not show any notable protein kinase binding at a concentration of 1 μM as verified in an active-site-directed competition binding assay against a panel of 457 kinases (see the Supporting Information).[17,18] Furthermore, profiling of **4** at 10 μM against 191 protein ATP binding sites confirmed the high selectivity of **4**; besides MTH1 only deoxycytidine kinase showed signficant binding (>50% inhibition of the reactive acyl phosphate ATP probe; see the Supporting Information).

In summary, we have described the discovery of the first small-molecule inhibitor of the repair enzyme 8-oxo-dGTPase (MTH1). The inhibitor is not a canonical small organic molecule but rather an unconventional cyclometalated ruthenium half-sandwich complex. The organometallic inhibitor **4** with activity in the low-nanomolar range displays an astonishing specificity, as verified with an extended panel of protein kinases and other ATP binding proteins. These results reinforce conclusions drawn from our previous work on metal-based inhibitors of protein kinases, namely, that inert metal complexes constitute excellent scaffolds for highly selective molecular probes, which we attribute to the limited flexibility of the globular metal complexes.[19] Furthermore, this work provides a blueprint for the discovery and development of organometallic inhibitors of other purine nucleotide binding proteins by using ruthenium-coordinated adenine and quinazoline derivatives with different coordination spheres. Finally, the novel organometallic MTH1 inhibitor **4** will be employed as a tool for the closer investigation of the biological function of MTH1 and its value as a target for anticancer therapy.

Received: September 6, 2013
Published online: November 20, 2013

**Keywords:** 7,8-dihydro-8-oxoguanosine triphosphatase · enzyme inhibitors · organometallic compounds · protein crystal structures · ruthenium

[1] The human purinome: a) T. A. J. Haystead, *Curr. Top. Med. Chem.* **2006**, *6*, 1117–1127; b) M. Knapp, C. Bellamacina, J. M. Murray, D. E. Bussiere, *Curr. Top. Med. Chem.* **2006**, *6*, 1129–1159; c) J. M. Murray, D. E. Bussiere, *Methods Mol. Biol.* **2009**, *575*, 47–92.

[2] For applications of metal-containing compounds in the life sciences, see: a) R. H. Fish, G. Jaouen, *Organometallics* **2003**, *22*, 2166–2177; b) *Bioorganometallics* (Ed.: G. Jaouen), Wiley-VCH, Weinheim, **2005**; c) M. J. Hannon, *Chem. Soc. Rev.* **2007**, *36*, 280–295; d) R. Alberto, *J. Organomet. Chem.* **2007**, *692*, 1179–1186; e) B. M. Zeglis, V. C. Pierre, J. K. Barton, *Chem. Commun.* **2007**, 4565–4579; f) T. W. Hambley, *Science* **2007**, *318*, 1392–1393; g) T. W. Hambley, *Dalton Trans.* **2007**, 4929–4937; h) A. Levina, A. Mitra, P. A. Lay, *Metallomics* **2009**, *1*, 458–470; i) F. R. Keene, J. A. Smith, J. G. Collins, *Coord. Chem. Rev.* **2009**, *253*, 2021–2035; j) K. L. Haas, K. J. Franz, *Chem. Rev.* **2009**, *109*, 4921–4960; k) U. Schatzschneider, *Eur. J. Inorg. Chem.* **2010**, 1451–1467; l) C.-M. Che, F.-M. Siu, *Curr. Opin. Chem. Biol.* **2010**, *14*, 255–261; m) G. Gasser, I. Ott, N. Metzler-Nolte, *J. Med. Chem.* **2011**, *54*, 3–25; n) E. A. Hillard, G. Jaouen, *Organometallics* **2011**, *30*, 20–27; o) E. Meggers, *Angew. Chem.* **2011**, *123*, 2490–2497; *Angew. Chem. Int. Ed.* **2011**, *50*, 2442–2448; p) M. Rouffet, S. M. Cohen, *Dalton Trans.* **2011**, *40*, 3445–3454; q) L. Salassa, *Eur. J. Inorg. Chem.* **2011**, 4931–4947; r) A. Bergamo, G. Sava, *Dalton Trans.* **2011**, *40*, 7817–7823; s) M. Patra, G. Gasser, *ChemBioChem* **2012**, *13*, 1232–1252; t) Z. T. Ball, *Acc. Chem. Res.* **2013**, *46*, 560–570; u) C. G. Hartinger, N. Metzler-Nolte, P. J. Dyson, *Organometallics* **2012**, *31*, 5677–5685; v) P. K. Sasmal, C. N. Streu, E. Meggers, *Chem. Commun.* **2013**, *49*, 1581–1587; w) N. P. E. Barry, P. J. Sadler, *Chem. Commun.* **2013**, *49*, 5106–5131; x) N. L. Kilah, E. Meggers, *Aust. J. Chem.* **2012**, *65*, 1325–1332; y) K. J. Kilpin, P. J. Dyson, *Chem. Sci.* **2013**, *4*, 1410–1419.

[3] E. Meggers, G. E. Atilla-Gokcumen, H. Bregman, J. Maksimoska, S. P. Mulcahy, N. Pagano, D. S. Williams, *Synlett* **2007**, 1177–1189.

[4] P. Chène, *Nat. Rev. Drug Discovery* **2002**, *1*, 665–673.

[5] Y. Nakabeppu, S. Oka, Z. Sheng, D. Tsuchimoto, K. Sakumi, *Mutat. Res.* **2010**, *703*, 51–58.

[6] a) M. P. Patricelli, A. K. Szardenings, M. Liyanage, T. K. Nomanbhoy, M. Wu, H. Weissig, A. Aban, D. Chun, S. Tanner, J. W. Kozarich, *Biochemistry* **2007**, *46*, 350–358; b) M. P. Patricelli, T. K. Nomanbhoy, J. Wu, H. Brown, D. Zhou, J. Zhang, S. Jagannathan, A. Aban, E. Okerberg, C. Herring, B. Nordin, H. Weissig, Q. Yang, J. D. Lee, N. S. Gray, J. W. Kozarich, *Chem. Biol.* **2011**, *18*, 699–710.

[7] Complex **4** is stable in [$D_6$]DMSO/$D_2O$ (9:1; 5 mM) at room temperature in the presence of an equimolar amount of 2-mercaptoethanol for at least seven days as has been verified by $^1$H NMR spectroscopy.

[8] J. E. Garbarino, I. R. Gibbons, *BMC Genomics* **2002**, *3*, 18.

[9] H. Kim, R. E. Kelly, D. R. Evans, *J. Biol. Chem.* **1992**, *267*, 7177–7184.

[10] L. M. Svensson, A.-S. Jemth, M. Desroses, O. Loseva, T. Helleday, M. Högbom, P. Stenmark, *FEBS Lett.* **2011**, *585*, 2617–2621.

[11] For a solution structure of MTH1, see: M. Mishima, Y. Sakai, N. Itoh, H. Kamiya, M. Furuichi, M. Takahashi, Y. Yamagata, S. Iwai, Y. Nakabeppu, M. Shirakawa, *J. Biol. Chem.* **2004**, *279*, 33806–33815.

[12] a) K. Fujikawa, H. Kamiya, H. Yakushiji, Y. Fujii, Y. Nakabeppu, H. Kasai, *J. Biol. Chem.* **1999**, *274*, 18201–18205; b) K. Fujikawa, H. Kamiya, H. Yakushiji, Y. Nakabeppu, H. Kasai, *Nucleic Acids Res.* **2001**, *29*, 449–454.

[13] For cocrystal structures of organometallic half-sandwich and sandwich compounds bound noncovalently to proteins, see: a) J. É. Debreczeni, A. N. Bullock, G. E. Atilla, D. S. Williams, H. Bregman, S. Knapp, E. Meggers, *Angew. Chem.* **2006**, *118*, 1610–1615; *Angew. Chem. Int. Ed.* **2006**, *45*, 1580–1585; b) N. Pagano, J. Maksimoska, H. Bregman, D. S. Williams, R. D. Webster, F. Xue, E. Meggers, *Org. Biomol. Chem.* **2007**, *5*, 1218–1227; c) J. Maksimoska, L. Feng, K. Harms, C. Yi, J. Kissil, R. Marmorstein, E. Meggers, *J. Am. Chem. Soc.* **2008**, *130*, 15764–15765; d) G. E. Atilla-Gokcumen, N. Pagano, C. Streu, J. Maksimoska, P. Filippakopoulos, S. Knapp, E. Meggers, *ChemBioChem* **2008**, *9*, 2933–2936; e) P. Xie, D. S. Williams, G. E. Atilla-Gokcumen, L. Milk, M. Xiao, K. S. Smalley, M. Herlyn, E. Meggers, R. Marmorstein, *ACS Chem. Biol.* **2008**, *3*, 305–316; f) P. Xie, C. Streu, J. Qin, H. Bregman, N. Pagano, E. Meggers, R. Marmorstein, *Biochemistry* **2009**, *48*, 5187–5198; g) A. N. Bullock, S. Russo, A. Amos, N. Pagano, H. Bregman, J. É. Debreczeni, W. H. Lee, F. von Delft, E. Meggers, S. Knapp, *PLoS One* **2009**, *4*, e7112; h) G. E. Atilla-Gokcumen, L. Di Constanzo, E. Meggers, *J. Biol. Inorg. Chem.* **2011**, *16*, 45–50; i) S. Blanck, Y. Geisselbrecht, K. Kräling, S. Middel, T. Mietke, K. Harms, L.-O. Essen, E. Meggers, *Dalton Trans.* **2012**, *41*, 9337–9348; j) A. J. Salmon, M. L. Williams, A. Hofmann, S.-A. Poulsen, *Chem. Commun.* **2012**, *48*, 2328–2330; k) D. Can, B.

  

Spingler, P. Schmutz, F. Mendes, P. Raposinho, C. Fernandes, F. Carta, A. Innocenti, I. Santos, C. T. Supuran, R. Alberto, *Angew. Chem.* **2012**, *124*, 3410 – 3413; *Angew. Chem. Int. Ed.* **2012**, *51*, 3354 – 3357.

[14] A. S. Mildvan, Z. Xia, H. F. Azurmendi, V. Saraswat, P. M. Legler, M. A. Massiah, S. B. Gabelli, M. A. Bianchet, L.-W. Kang, L. M. Amzel, *Arch. Biochem. Biophys.* **2005**, *433*, 129 – 143.

[15] The absolute configuration at the ruthenium center was assigned according to the priority order of the ligands: Cp > N > CO > C.

[16] The interaction surface was calculated using PISA (PDBe PISA v1.47) as accessible via http://pdbe.org/pisa. The given value is the average of the interaction interfaces obtained from the two complexes in the asymmetric unit.

[17] a) M. A. Fabian, W. H. Biggs III, D. K. Treiber, C. E. Atteridge, M. D. Azimioara, M. G. Benedetti, T. A. Carter, P. Ciceri, P. T. Edeen, M. Floyd, J. M. Ford, M. Galvin, J. L. Gerlach, R. M. Grotzfeld, S. Herrgard, D. E. Insko, M. A. Insko, A. G. Lai, J.-M. Lélias, S. A. Mehta, Z. V. Milanov, A. M. Velasco, L. M. Wodicka, H. K. Patel, P. P. Zarrinkar, D. J. Lockhardt, *Nat. Biotechnol.* **2005**, *23*, 329 – 336; b) M. W. Karaman, S. Herrgard, D. K. Treiber, P. Gallant, C. E. Atteridge, B. T. Campbell, K. W. Chan, P. Ciceri, M. I. Davis, P. T. Edeen, R. Faraoni, M. Floyd, J. P. Hunt, D. J. Lockhardt, Z. V. Milanov, M. J. Morrison, G. Pallares, H. K. Patel, S. Pritchard, L. M. Wodicka, P. P. Zarrinkar, *Nat. Biotechnol.* **2008**, *26*, 127 – 132.

[18] This might result at least in part from the additional methyl substituent at C2 which sterically disturbs the hydrogen bonding between inhibitor and the backbone of the hinge region of protein kinases. In contrast, in the case of MTH1 even an ethyl substituent is tolerated without significant loss of affinity (see the Supporting Information).

[19] a) L. Feng, Y. Geisselbrecht, S. Blanck, A. Wilbuer, G. E. Atilla-Gokcumen, P. Filippakopoulos, K. Kräling, M. A. Celik, K. Harms, J. Maksimoska, R. Marmorstein, G. Frenking, S. Knapp, L.-O. Essen, E. Meggers, *J. Am. Chem. Soc.* **2011**, *133*, 5976 – 5986; b) S. Blanck, J. Maksimoska, J. Baumeister, K. Harms, R. Marmorstein, E. Meggers, *Angew. Chem.* **2012**, *124*, 5335 – 5338; *Angew. Chem. Int. Ed.* **2012**, *51*, 5244 – 5246.

  